Naunyn-Schmiedeberg's Arch Pharmacol (2011) 384:287–299
DOI 10.1007/s00210-011-0671-5

ORIGINAL ARTICLE

N^{α}-Methylated phenylhistamines exhibit affinity to the hH_4R—a pharmacological and molecular modelling study

Hans-Joachim Wittmann · Sigurd Elz · Roland Seifert · Andrea Straßer

Received: 19 May 2011 / Accepted: 8 July 2011 / Published online: 29 July 2011

Abstract Histamine H_1-receptor agonists and antagonists exhibit affinity to the human histamine H_4-receptor (hH_4R). However, the pharmacological profiles between hH_1R and hH_4R exhibit similarities and differences. Since supra-histaprodifen and trifluoromethylphenylhistamine show significant affinity to hH_4R, the aim of this study was to analyse a large number of new phenylhistamines, histaprodifens and phenoprodifens at hH_4R to extend the pharmacological profile of these compound classes at hH_4R. The hH_4R-RGS19 fusion protein was co-expressed with $G_{\alpha i2}$ and $G_{\beta 1\gamma 2}$ in Sf9 insect cells, and [^{3}H]histamine competition binding as well as GTPase assays were performed. Based on adequate crystal structures, homology models of hH_4R were generated. Molecular modelling studies, including molecular dynamics and prediction of Gibbs energy of ligand binding, were performed in order to explain the pharmacological data at hH_4R on molecular level. The exchange of the phenyl moiety of phenylhistamines into the diphenylpropyl moiety of histaprodifens acts, in contrast to hH_1R, as partial agonism–inverse agonism switch at hH_4R. Based on our studies, some phenylhistamine derivatives with significantly higher affinity at hH_4R than at hH_1R were identified. The molecular dynamic simulations revealed two different conformations for the highly conserved $Trp^{6.48}$, suggested to be involved in receptor activation. Furthermore, the predicted Gibbs energy of ligand binding for six selected phenylhistamines was in very good agreement with the experimentally determined affinities. We identified phenylhistamine derivatives with higher affinity at hH_4R than at hH_1R. Besides, we have identified partial agonism–inverse agonism switch between phenylhistamines and histaprodifens at hH_4R. These results are very important to understand selectivity between hH_1R and hH_4R and to design new potent H_1R and/or H_4R receptor ligands.

Keywords Histamine H_1 receptor · Histamine H_4 receptor · Gibbs energy · Phenylhistamines · Histaprodifens

Abbreviations

cpd	Compound
h	Human
H_1R	Histamine H_1 receptor
H_4R	Histamine H_4 receptor
n. d.	Not determined
TM	Transmembrane Domain

Introduction

Histamine is a biogenic amine and mediates physiological and pathophysiological effects via four histamine receptor

We dedicate this paper to the late Prof. Dr. Dr. Dr. h.c. Walter Schunack who developed phenylhistamines and histaprodifens.

Electronic supplementary material The online version of this article (doi:10.1007/s00210-011-0671-5) contains supplementary material, which is available to authorized users.

H.-J. Wittmann
Faculty of Chemistry and Pharmacy, University of Regensburg, 93040, Regensburg, Germany

S. Elz
Department of Pharmaceutical/Medicinal Chemistry I, School of Pharmacy, University of Regensburg, 93040, Regensburg, Germany

R. Seifert
Institute of Pharmacology, Medical School of Hannover, 30625, Hannover, Germany

A. Straßer (✉)
Department of Pharmaceutical/Medicinal Chemistry II, School of Pharmacy, University of Regensburg, 93040, Regensburg, Germany
e-mail: andrea.strasser@chemie.uni-regensburg.de

subtypes (Foord et al. 2005). The histamine H_1 receptor (H_1R) is involved in allergic reactions, the H_2R is involved in secretion of gastric acid, the H_3R is responsible for modulation of neurotransmitter release and the histamine H_4 receptor (H_4R) acts as an immunomodulator (de Esch et al. 2005; Thurmond et al. 2008). Recent studies support the hypothesis that the H_1R and H_4R possess a synergistic role in treatment of type-I allergic reactions (Thurmond et al. 2008; Deml et al. 2009). Thus, a detailed study of H_1 and H_4 receptor ligands at both H_1R and H_4R is necessary. Furthermore, such studies provide a more detailed insight into the interaction between ligand and receptor on molecular level. Besides, the understanding with regard to receptor subtype selectivity will be increased.

A wide variety of structurally diverse agonists (Hashimoto et al. 2003; Lim et al. 2005; Igel et al. 2009; Smits et al. 2009) and antagonists (Jablonowski et al. 2003; Terzioglu et al. 2004; Thurmond et al. 2004; Venable et al. 2005; Smits et al. 2008, 2009) at the histamine H_4 receptor have been identified. A recent study (Deml et al. 2009) has shown that phenylhistamines and suprahistaprodifen, previously classified as "selective H_1R agonists" (Leschke et al. 1995; Elz et al. 2000; Menghin et al. 2003; Seifert et al. 2003; Straßer et al. 2008, 2009), exhibit affinity to the human (h)H_4R. The aim of this study was to analyse the interactions of phenylhistamines and histaprodifens between hH_1R and hH_4R in more detail. Therefore, we analysed several new phenylhistamine and histaprodifen derivatives as well as phenoprodifens at the hH_4R (Fig. 1).

To study the pharmacology of phenylhistamines and histaprodifens at hH_4R, we co-expressed hH_4R-RGS19 with $G_{\alpha i2}$ and $G_{\beta 1\gamma 2}$ in Sf9 insect cells (Deml et al. 2009; Schneider et al. 2010). For pharmacological characterization, [^{3}H]histamine competition binding assays and steady-state GTPase assays were performed. In order to obtain information about the binding mode of phenylhistamines and histaprodifens at hH_4R, phenylhistamines were docked into the active and histaprodifen into the inactive state model of hH_4R. Subsequently, molecular dynamic simulations, including the surrounding of the receptor, were performed. Additionally, we performed calculations of $\Delta\Delta G°_{solv}$(water→binding pocket of hH_4R), corresponding to the transfer of a ligand from the aqueous phase into the binding pocket of hH_4R, for six selected phenylhistamines.

Materials and methods

Materials [γ-^{32}P]GTP was synthesized as described (Preuss et al. 2007). [^{3}H]Histamine (14.2 Ci/mmol) was from PerkinElmer Life Sciences (Boston, MA, USA). As liquid scintillation cocktail, Rotiszint ecoplus from Roth (Karlsruhe, Germany) was used. Phenylhistamines, histaprodifens and phenoprodifens were synthesized as described (Straßer et al. 2008, 2009). Sources of all other materials were described earlier (Seifert et al. 2003; Straßer et al. 2008).

Preparation of compound stock solutions Chemical structures of the analysed compounds are given in Fig. 1. Compounds **1**–**30** were dissolved as described (Straßer et al. 2008, 2009). The final DMSO concentration in all assays was adjusted to 3% (*v*/*v*) or 5% (*v*/*v*), as appropriate for the ligands. Control experiments with histamine, dissolved in double-distilled water or dissolved in a solvent containing 50% (*v*/*v*) DMSO and 50% (*v*/*v*) double-distilled water, showed that a final DMSO concentration of 5% (*v*/*v*) did not shift pK_i and pEC_{50} values of histamine.

Pharmacological and biochemical methods Construction of baculoviruses was described earlier (Kelley et al. 2001; Seifert et al. 2003; Straßer et al. 2008; Schneider et al. 2010). Cell culture, membrane preparation and determination of protein concentration were performed as described previously (Seifert et al. 2003; Straßer et al. 2008). All assays were performed with Sf9 insect cell membranes, coexpressing hH_4R-RGS19, $G_{\alpha i2}$ and $G_{\beta 1\gamma 2}$. Ligand concentrations were used in the range from 0.1 nM up to 316 μM, where appropriate. Competition binding assay and steady-state GTPase assay were performed as described (Straßer et al. 2008; Schneider et al. 2010). Shortly, competition binding assays were performed in the presence of 10 nM [^{3}H]histamine. Reaction mixtures were incubated for 90 min at room temperature and shaking at 250 rpm. Bound [^{3}H]histamine was determined by filtration through GF/C filters and liquid scintillation counting. The steady-state GTPase assays were performed in the agonist mode as described (Straßer et al. 2008). [^{35}S]GTPγS binding assays were performed, as described (Schneider et al. 2009). Shortly, the studies were conducted in presence of 2 nM [^{35}S]GTPγS, 1 μM GDP and 100 mM NaCl. Incubations were conducted for 120 min at room temperature and at 250 rpm. All samples were filtered through GF/C filters and bound [^{35}S]GTPγS was determined by liquid scintillation counting. For data analysis, the software Prism 4.02 (GraphPad Software Inc., San Diego, CA, USA) was used. pK_i values were calculated according to Cheng and Prusoff (1973). All data are the means±SEM of at least three independent experiments. For comparison of two pairs of data, the significance of the deviation of zero p was calculated using the t test.

Molecular modelling The inactive state model of hH_4R was constructed by homology modelling using SYBYL 7.0 (Tripos Inc.) as described (Deml et al. 2009). For construction of the active state model, the crystal structure

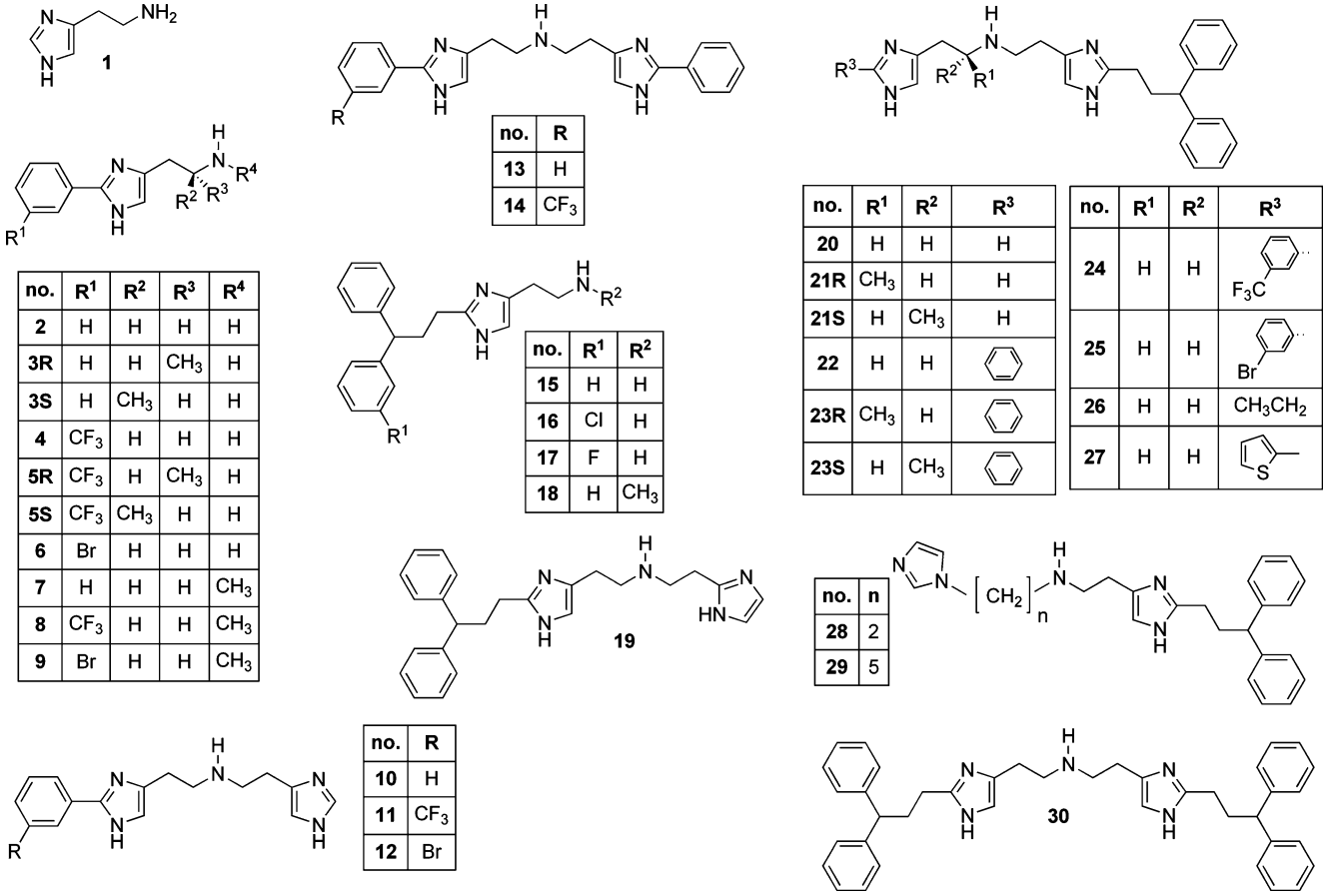

Fig. 1 Structures of histamine, phenylhistamines, histaprodifens and phenoprodifens. Histamine **1**, small phenylhistamines **2**–**9**, bulky phenylhistamines with an additional histamine moiety **10**–**12**, dimeric phenylhistamines **13** and **14**, small histaprodifens **15**–**18**, bulkier histaprodifens **19**, **26**–**29**, suprahistaprodifens **20**–**21**, phenoprodifens **22**–**25**, dimeric histaprodifen **30**

of opsin 3DQB (Scheerer et al. 2008) was used as template. For a detailed explanation, see Supplementary material. Phenylhistamines **2**, **4**, **6**–**9** were docked manually in the binding pocket of the hH_4R active state model, whereas the histaprodifen **15** was docked into the binding pocket of the hH_4R inactive state model. Subsequently, molecular dynamic simulations with the software package GROMACS 4.0.2 (Van der Spoel et al. 2005) were carried out. For the receptor, the ffG53A6 force field (Oostenbrink et al. 2004) was used. The GROMACS topologies for the ligands **2**, **4**, **6**–**9** were calculated using the PRODRG server (http://davapc1.bioch.dundee.ac.uk/prodrg/) (Schuettelkopf and van Allten 2004). For partial charges of the ligands, Gasteiger–Hückel partial charges were used. The equilibration phase and the productive phase were performed, using the system and simulation parameters, as described (Straßer et al. 2008). For calculation of $\Delta G°_{sol}$(ligand in water) and $\Delta G°_{sol}$(ligand in binding pocket of hH_4R), we also used GROMACS 4.0.2 using thermodynamic integration (Straatsma and Mc Cammon 1991; Villa and Mark 2002). We performed calculations, using the following values for the coupling parameter λ, which switches the interaction between ligand and surrounding on or off, respectively: 0.0, 0.05, 0.1, 0.2, 0.3, 0.4, 0.45, 0.5, 0.55, 0.6, 0.7, 0.8, 0.9, 0.95, 0.975, 0.99, 0.995 and 1.0. To avoid abrupt transitions from one λ to the next λ, we used small steps in increasing λ. In order to achieve an acceptable simulation time, simulation times of 100 ps for each λ were used. For calculation of $\Delta G°_{sol}$(L, wat), describing the Gibbs energy of solvation of the ligand in water, and $\Delta G°_{sol}$(L, LR), describing the Gibbs energy of solvation of the ligand in the binding pocket of the ligand–receptor complex, each calculation was performed two times using different starting structures.

Prediction of thermodynamic data In general, for the binding of a ligand L into the binding pocket of a receptor R, an equilibrium between L and R on the one hand and the ligand–receptor complex LR on the other hand is defined:

$$L + R \rightleftharpoons LR \tag{1}$$

The corresponding $\Delta_R G°$ is given by the equation

$$\Delta_R G° = -RT\ln(K) \tag{2}$$

wherein K represents the association constant. Additionally, $\Delta_R G°$ can be described by the following equation:

$$\Delta_R G^\circ = G^\circ(LR) - G^\circ(L, wat) - G^\circ(R) \quad (3)$$

Therein, G°(LR) describes the Gibbs energy of the reference state for the ligand–receptor complex, G°(L, wat) describes the Gibbs energy of the reference state for the ligand solved in water and G°(R) describes the Gibbs energy of the reference state for the ligand-free receptor. These first two terms on the right-hand side of Eq. 3 are given by the following equations:

$$G^\circ(LR) = G^\circ(L, gas) + G^\circ(R, LR) + \Delta G^\circ_{sol}(L, LR) \quad (4)$$

and

$$G^\circ(L, wat) = G^\circ(L, gas) + \Delta G^\circ_{sol}(L, wat) \quad (5)$$

Therein, G°(L, gas) describes the Gibbs energy of reference state of the ligand in gas phase, G°(R, LR) describes the Gibbs energy of reference state of the receptor in the ligand-bound state, $\Delta G°_{sol}$(L, LR) describes the Gibbs energy of solvation of the ligand in the binding pocket of the ligand–receptor complex and $\Delta G°_{sol}$(L, wat) describes the Gibbs energy of solvation of the ligand in water.

Combining Eqs. 3, 4 and 5 results in the following equation:

$$\Delta_R G^\circ = G^\circ(R, LR) + \Delta G^\circ_{sol}(L, LR) - \Delta G^\circ_{sol}(L, wat) - G^\circ(R) \quad (6)$$

Molecular dynamics in combination with thermodynamic integration can be used to predict $\Delta G°_{sol}$(ligand in binding pocket of the receptor) and $\Delta G°_{sol}$(L, wat). Using these values, the change in Gibbs energy for the transfer of the ligand from the aqueous phase into the binding pocket of the receptor (hH_4R in this study), $\Delta\Delta G°_{sol}$(water→hH_4R) is given by

$$\Delta\Delta G^\circ_{sol}(water \rightarrow hH_4R) = \Delta G^\circ_{sol}(L, LR) - \Delta G^\circ_{sol}(L, wat) \quad (7)$$

Combining Eqs. 2, 6 and 7 leads to the following equation:

$$\Delta\Delta G^\circ_{sol}(water \rightarrow hH_4R) = -R\,T \times 2.303\ pK_i + G^\circ(R) - G^\circ(R, LR) \quad (8)$$

By fitting $\Delta\Delta G°_{sol}$(water→hH_4R) against the pK_i, a linearity, with the slope given by $-R\,T$×2.303 (corresponding to −5.7 kJ/mol for a temperature of 298.15 K) and the y-intercept given by G°(R)−G°(R, LR), should be received. Thus, Eq. 8 is suggested to be used to predict the change in Gibbs energy of the receptor during the process of ligand binding.

Results

Analysis of phenylhistamines, histaprodifens and phenoprodifens at hH_4R in the [^{3}H]histamine competition binding assay Tables 1 and 2 summarize the affinities of 33 studied compounds at hH_4R in the [^{3}H]histamine competition binding assay, and Fig. 2 shows representative competition binding isotherms. Phenylhistamine **2** showed low affinity at hH_4R. The introduction of an additional methyl group in R- **3R** and S-configuration **3S** decreased affinity, but there was no difference in affinity between **3R** and **3S**, as observed at hH_1R (Straßer et al. 2009). The introduction of a trifluoromethyl group in meta position **4** increased affinity compared to the unsubstituted phenylhistamine **2** (p=0.0009). But the introduction of an additional methyl group in R- **5R** and S-configuration **5S** significantly decreased affinity compared to **4** (p=0.087). The exchange of the trifluoromethyl group in **4** into a bromine **6** did not affect affinity. The N^α-methylated phenylhistamines **7**–**9** (Fig. 2a) showed a significant (**7** compared to **2**: p=0.0004; **8** compared to **4**: p=0.0129; **9** compared to **6**: p=0.0004) increase in affinity compared to the unmethylated compounds **2**, **4** and **6**. The affinity of phenylhistamine with an additional histamine moiety **10** was increased compared to the small phenylhistamine **2** (p=0.0007). The affinities of the derivatives with a trifluoromethyl group **11** or a bromine **12** were in the same range as for compound **10**. For the dimeric phenylhistamine **13**, a pK_i value in the range of phenylhistamine **2** was observed. The introduction of one trifluoromethyl moiety into dimeric phenylhistamine **14** slightly increased affinity (p=0.01).

The affinity of histaprodifen **15** was in the same range as for phenylhistamine **2**. The introduction of a chlorine **16** or fluorine **17** into one phenyl moiety did not lead to differences in affinity. The introduction of a methyl group in N^α position of histaprodifen **18** increased affinity (p=0.0045). Histaprodifen derivative **19** exhibited an affinity in the same range as **18**. Thus, the additional imidazolyl moiety had no significant influence onto affinity. The affinity of suprahistaprodifen **20** was in the same range as for phenylhistamine with an additional histamine moiety **10**. The introduction of a centre of chirality by a methyl group in compounds **21R** and **21S** led to a slight decrease in affinity, compared to suprahistaprodifen **20** (p=0.0027). Compared to suprahistaprodifen **20**, the affinity of phenoprodifen **22** to hH_4R was decreased (p=0.0034). The additional methyl moiety in R- **23R** and S-configuration **23S** did not substantially alter pK_i values compared to the unsubstituted compound **22**. However, the introduction of a trifluoromethyl group **24** into the phenylhistamine moiety of the unsubstituted phenoprodifen **22** showed a significant (p=0.017) increase in affinity, whereas the exchange of this trifluoromethyl group to a bromine **25** decreased affinity

Table 1 Affinities, potencies and efficacies of histamine, phenylhistamines, histaprodifens and phenoprodifens at hH_4R-RGS19 co-expressed with $G_{\alpha i2}$ and $G_{\beta 1\gamma 2}$ in Sf9 cell membranes in the competition binding and steady-state GTPase assay

cpd.	pK_i	pEC_{50}	E_{max}
1[a]	8.07±0.14	7.93±0.06	1.00
2[a]	4.79±0.04	4.92±0.07	0.32±0.03
3R	4.37±0.05	n. d.	−0.08±0.04
3S	4.26±0.08	n. d.	0.01±0.03
4[a]	5.91±0.12	5.83±0.08	0.51±0.02
5R	4.29±0.12	n. d.	−0.06±0.08
5S	4.58±0.29	n. d.	0.02±0.06
6[a]	5.76±0.01	5.02±0.03	0.67±0.01
10	5.77±0.08	5.75±0.03	0.80±0.10
11	5.47±0.09	5.39±0.11	0.11±0.10
12	5.98±0.16	5.31±0.13	0.32±0.05
13	4.49±0.05	n. d.	0.03±0.04
14	5.06±0.12	4.99±0.50	0.12±0.01
15	4.56±0.08	4.44±0.10	−0.48±0.08
16	4.76±0.09	4.57±0.01	−0.58±0.01
17	4.42±0.05	5.08±0.09	−0.36±0.10
18[a]	5.17±0.05	5.20±0.11	−0.64±0.03
19	5.21±0.12	n. d.	−0.03±0.03
20[a]	5.77±0.05	5.82±0.12	0.25±0.02
21R	5.37±0.03	4.99±0.05	−0.45±0.04
21S	5.06±0.08	5.17±0.11	−0.51±0.08
22	4.95±0.11	4.60±0.13	−0.63±0.03
23R	4.96±0.06	n. d.	< −0.21±0.09[b]
23S	4.93±0.07	n. d.	< −0.30±0.08[b]
24	5.68±0.15	5.79±0.18	0.35±0.07
25	5.04±0.13	n. d.	−0.02±0.01
26	4.73±0.02	5.23±0.05	0.91±0.04
27	5.22±0.01	5.10±0.54	−0.15±0.03
28	4.47±0.17	n. d.	−0.03±0.03
29	5.00±0.09	4.90±0.07	−0.53±0.08
30[a]	5.57±0.08	4.81±0.01	−0.88±0.02

[^{3}H]Histamine competition binding in Sf9 membranes expressing hH_4R-RGS19, $G_{\alpha i2}$ and $G_{\beta 1\gamma 2}$ was determined in presence of 10 nM [^{3}H]histamine as described under "Materials and methods". Data were analysed by nonlinear regression and were best fit to one-site (monophasic) competition curves. pK_i values were calculated according to Cheng and Prusoff (1973). The GTPase experiments were performed as described under "Materials and methods". Data were analysed by nonlinear regression and were best fit to sigmoidal concentration–response curves. The efficacy (E_{max}) of histamine was set 1.00. The E_{max} values of all other compounds were referred to this value. Data shown are means±SEM of at least three experiments performed in duplicates or triplicates each. Membranes were used from independent preparations

[a] Data already published (Deml et al. 2009). However, the data published in Deml et al. (2009) and the data presented in this study were actually generated at the same time and in parallel so that the reference to "historical" data is appropriate

[b] A decrease in efficacy was only observed for the highest analysed concentration of 100 μM

Table 2 Affinities of phenylhistamines **7**, **8** and **9** at hH_1R compared to hH_4R

cpd.	pK_i (hH_1R)	pK_i (hH_4R)	p (hH_1R versus hH_4R)
7[a]	5.17±0.09	6.13±0.08	0.0013
8[a]	5.58±0.06	6.80±0.04	<0.0001
9[a]	5.66±0.05	6.56±0.06	0.0003

Affinities of **7**, **8** and **9** were already determined previously by [^{3}H]Mepyramine competition binding in Sf9 membranes expressing hH_1R (Straßer and Wittmann 2010). [^{3}H]Histamine competition binding in Sf9 membranes expressing hH_4R-RGS19, $G_{\alpha i2}$ and $G_{\beta 1\gamma 2}$ was determined in presence of 10 nM [^{3}H]histamine as described under "Materials and methods". Data were analysed by nonlinear regression and were best fit to one-site (monophasic) competition curves. pK_i values were calculated according to Cheng and Prusoff (1973). Data shown are means±SEM of at least three experiments performed in duplicates or triplicates each. Membranes were used from independent preparations

[a] Affinities of **7**–**9** at hH_1R were already published previously (Straßer and Wittmann 2010)

(p=0.038), comparable to phenoprodifen **22**. An additional ethyl moiety in **26** compared to suprahistaprodifen **20** substantially decreased affinity (p=0.0001), whereas an additional thienyl moiety in **27** compared to suprahistaprodifen **20** led only to a smaller decrease in affinity. Compounds **28** and **29**, possessing a different substitution pattern of the terminal imidazolyl moiety, compared to suprahistaprodifen **20**, in combination with a varying length of the CH_2-spacer, showed a decreased affinity compared to **20**. Dimeric histaprodifen **30** showed an increase in pK_i value, compared to histaprodifen **15**.

Analysis of phenylhistamines, histaprodifens and phenoprodifens at hH_4R in the functional steady-state GTPase and GTPγS binding assay In Tables 1, 3 and Fig. 2b, the potencies and efficacies of the analysed compounds are given. As well-known (Deml et al. 2009), histamine **1** showed a high potency at hH_4R. The potency as well as the efficacy of phenylhistamine **2** was decreased, compared to histamine **1**. The chiral phenylhistamines **3R** and **3S** behaved as neutral antagonists. The trifluoromethyl group in *meta* position of the phenyl moiety **4** increased potency (p=0.0015) as well as efficacy (p=0.01) compared to the unsubstituted phenylhistamine **2**. The chiral derivatives **5R** and **5S** exhibited antagonism. The exchange of the trifluoromethyl **4** into a bromine **6** did not result in differences in efficacy, but potency decreased significantly (p=0.0006). The more bulky phenylhistamine with an additional histamine moiety **10** showed, compared to phenylhistamine **2**, a significantly higher potency (p=0.0005) and efficacy (p=0.0072). But in contrast to compounds **2** and **4**, the introduction of a trifluoromethyl group into **10**, leading to **11**, decreased potency and efficacy

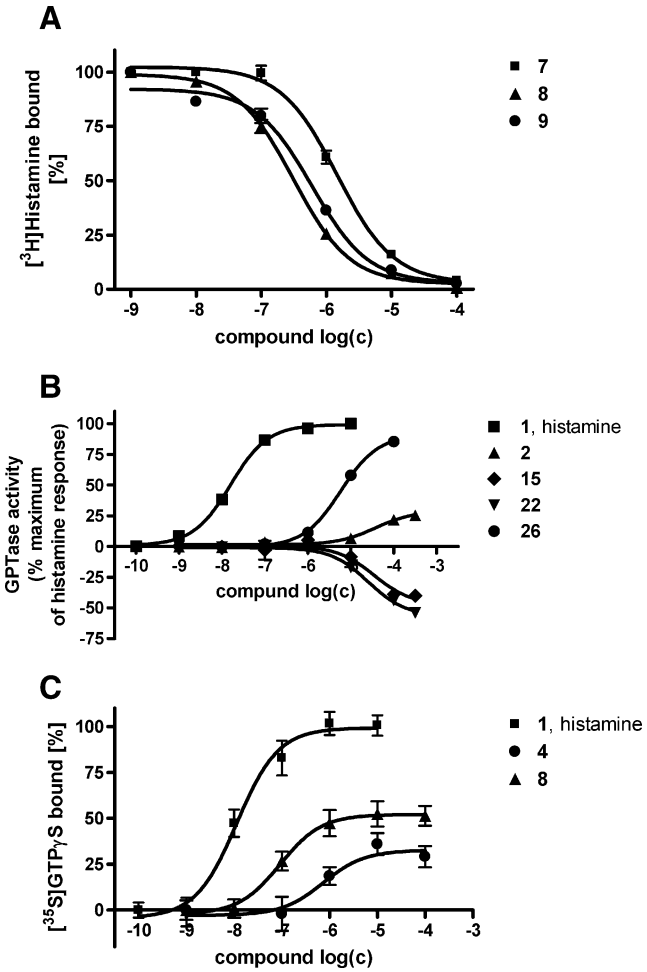

Fig. 2 Competition binding isotherms and concentration–response curves for selected phenylhistamines and histaprodifens at hH_4R. The experiments were performed using Sf9 cell membranes expressing hH_4R-RGS19, $G_{\alpha i2}$ and $G_{\beta 1\gamma 2}$ as described under "Materials and methods". Data were analysed by nonlinear regression and were best fit to one-site (monophasic) competition curves. **a** Competition binding isotherms; the experiments were performed in presence of 10 nM [^{3}H]histamine; **b** concentration response curves determined in the steady-state GTPase assay; **c** [^{35}S]GTPγS binding curves for histamine **1** and phenylhistamines **4** and **8**

(p=0.0045). The exchange of the trifluoromethyl group in **11** into bromine **12** did not affect potency and slightly increased efficacy. Dimeric phenylhistamine **13** showed antagonism, but the introduction of a trifluoromethyl moiety in **14** slightly increased efficacy.

The potency of histaprodifen **15** was in the same range as for phenylhistamine **2**. However, in contrast to phenylhistamine **2**, histaprodifen **15** was an inverse agonist. The introduction of chlorine into one phenyl moiety of the histaprodifen **16** did not affect potency and efficacy, compared to histaprodifen **15** itself. In contrast, fluorine at the corresponding position **17** showed, compared to histaprodifen **15**, an increase in potency (p=0.01). Compared to histaprodifen **15**, for the N^{α}-methylated derivative **18**, a significant increase in potency (p=0.0082) and a decrease in efficacy were observed. Histaprodifen derivative **19** with an additional imidazolyl moiety showed antagonistic behaviour. A different substitution pattern of this imidazolyl moiety, as given for suprahistaprodifen **20**, significantly increased efficacy (p=0.005). The potency of suprahistaprodifen **20** was higher than for histaprodifen **15** (p=0.001). The chiral suprahistaprodifens **21R** and **21S** with an additional methyl group, in contrast to suprahistaprodifen **20**, showed inverse agonism, and the potency decreased (p=0.037). There were no significant differences in potency and efficacy between **21R** and **21S**. Phenoprodifen **22**, possessing an additional phenyl moiety compared to suprahistaprodifen **20**, showed a decreased potency compared to **20** (p=0.024) and acted, in contrast to **20** as inverse agonist. For the chiral phenoprodifens **23R** and **23S**, weak inverse agonism was observed. The trifluoromethyl-substituted phenoprodifen **24** revealed, compared to phenoprodifen **22**, an increased potency (p= 0.0065) and the inverse agonism of **22** switched to partial agonism of **24**. The exchange of the trifluoromethyl group into a bromine **25** led to antagonistic behaviour. The additional ethyl moiety in **26** decreased potency but increased efficacy compared to suprahistaprodifen **20**. The additional thienyl moiety of **27** did not affect potency but switched the large partial agonism of **26** into inverse agonism. The histaprodifen derivatives **28** and **29** showed antagonistic or inverse agonistic behaviour, respectively. Dimeric histaprodifen **30**, compared to suprahistaprodifen **20**, showed a decreased potency and acted, in contrast to **20**, as inverse agonist at hH_4R.

The pharmacological data of compounds **1**, **2**, **4**, **6**, **7**–**9** obtained with the [^{35}S]GTPγS binding assay are given in

Table 3 Potencies and efficacies of phenylhistamines **2**, **4**, **6**–**9** at hH_4R

cpd.	pEC_{50}	E_{max}
1	7.90±0.05	1.00
2	4.59±0.13	0.27±0.03
4	6.12±0.12	0.36±0.04
6	5.33±0.29	0.56±0.16
7	5.63±0.13	0.87±0.14
8	7.07±0.07	0.54±0.06
9	6.80±0.23	0.80±0.04

Functional binding assay with [^{35}S]GTPγS with Sf9 membranes, expressing hH_4R-RGS19, $G_{\alpha i2}$ and $G_{\beta 2\gamma 2}$ was determined, as described under "Materials and methods". Data were analysed by nonlinear regression and were best fit to sigmoidal concentration–response curves. The efficacy (E_{max}) of histamine was set 1.00. The E_{max} values of all other compounds were referred to this value. Data shown are means±SEM of at least three experiments performed in duplicates each. Membranes were used from independent preparations

Table 3. A comparison of potencies and efficacies of compounds **1**, **2**, **4** and **6** with the corresponding data, obtained in the steady-state GTPase assay (Table 1), shows a very good accordance. In another context, the good accordance between steady-state GTPase and GTPγS binding assay was shown previously (Seifert et al. 1998; Wenzel-Seifert and Seifert 2000). The functional data revealed a significantly higher potency (p=0.0052) and efficacy (p=0.011) for the N^{α}-methylated phenylhistamine **7**, compared to phenylhistamine **2** itself. A similar trend was observed for compounds **4** and **8**: Again, the N^{α}-methylated phenylhistamine derivative **8** showed a significantly higher potency (p=0.002) and efficacy (p=0.049), compared to the unmethylated derivative **4** (Fig. 2c). The bromine-substituted N^{α}-methylated phenylhistamine **9** exhibited a higher potency and efficacy as the bromine-substituted phenylhistamine **6**. To summarize the binding and functional data, structure–activity relationships of the most important phenylhistamines, histaprodifens, supra- and phenoprodifens at hH_4R is given in Fig. 3.

Binding mode of phenylhistamines **2**, **4**, **6**–**9** *and histaprodifen* **15** Representative binding modes of **2** and **8** and **15** at hH_4R are shown in Fig. 4. Phenylhistamine **2** (Fig. 4a) and **8** (Fig. 4c) fit into the binding pocket. However, only one electrostatic interaction between the positively charged amino moiety of phenylhistamine **2** or **8** and the highly conserved $Asp^{3.32}$ was detected. The imidazole and phenyl moieties of **2** or **8** are embedded in an aromatic pocket, established by $Tyr^{3.33}$, $Trp^{6.48}$ and $Tyr^{6.51}$. Stable hydrogen bonds between the imidazole moiety of the phenylhistamine and hH_4R were not observed during molecular dynamic simulation. However, the molecular modelling revealed two small empty pockets (Fig. 4a, arrows 1 and 2) in case of the smallest phenylhistamine **2**. In case of phenylhistamine derivative **8**, the additional methyl moiety fits into pocket 1 (Fig. 4a, c, arrow 1), whereas the trifluoromethyl group fits into pocket 2 (Fig. 4a, c, arrow 2). This results in an increase of interaction between hH_4R and phenylhistamine derivative **8**, compared to phenylhistamine **2**. Due to a free small pocket between the phenyl-

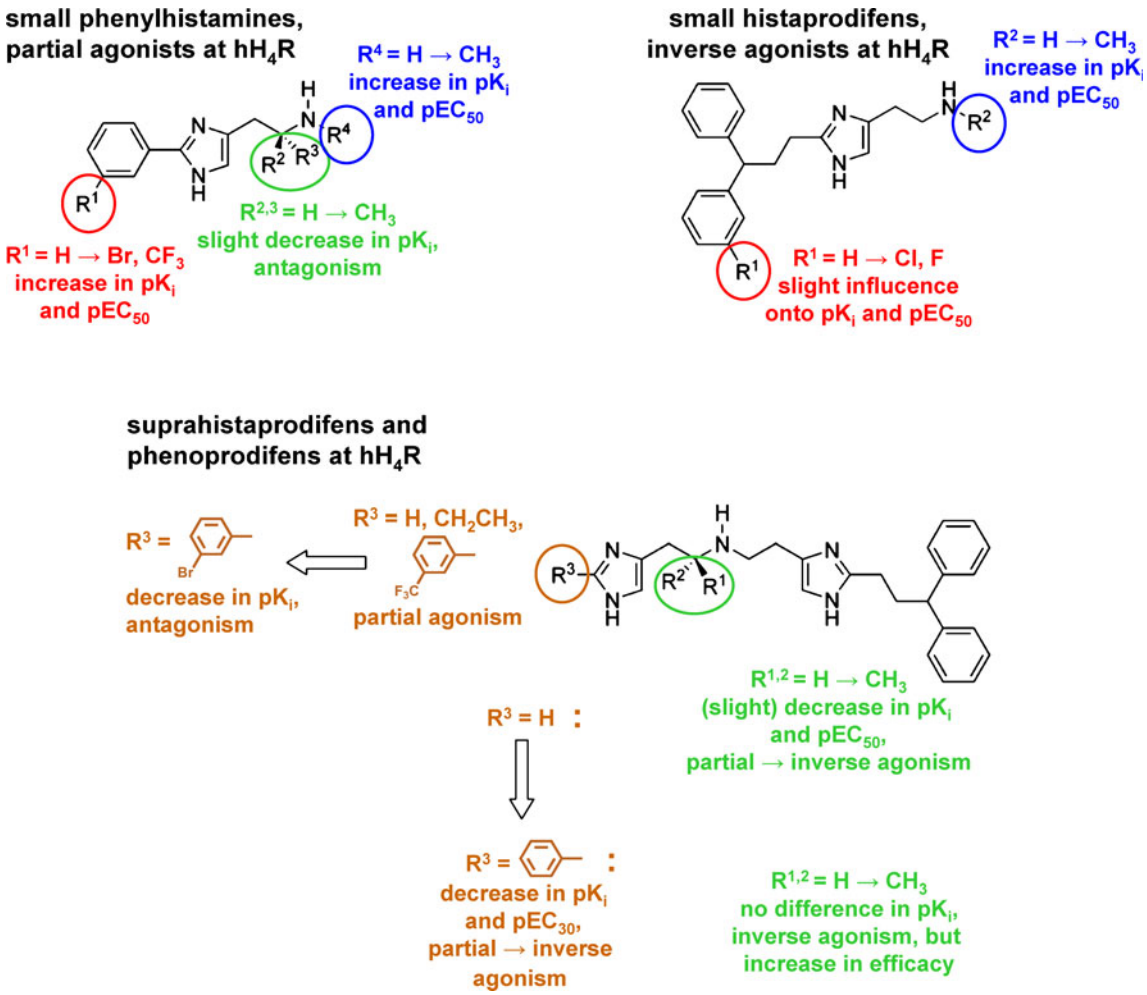

Fig. 3 Summary of the most important structure activity relationships of selected phenylhistamines, histaprodifens, supra- and phenoprodifens at hH_4R. The summary is based on the results, presented in Tables 1 2 and 3

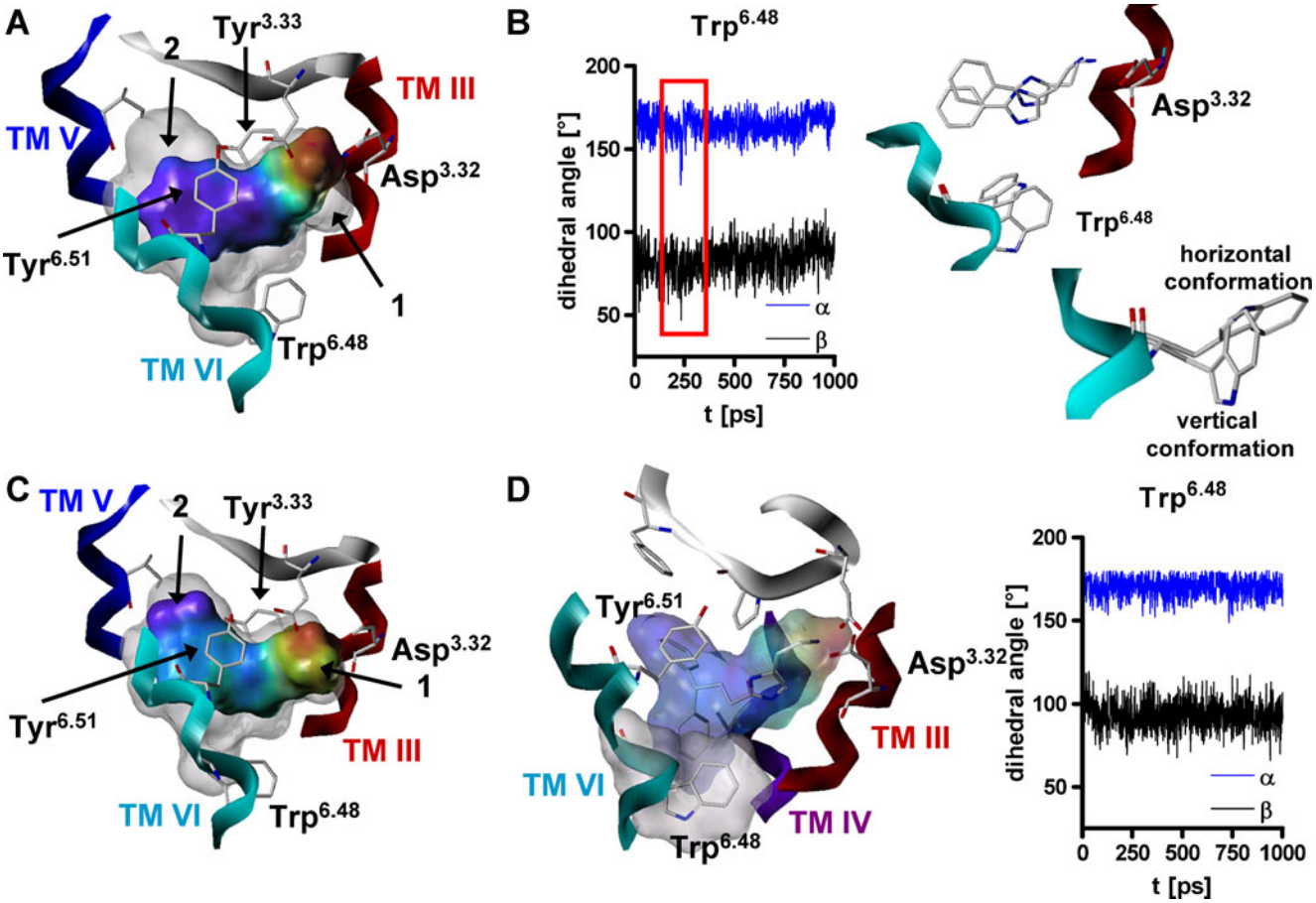

Fig. 4 Binding mode of phenylhistamines **2** and **8** and histaprodifen **15** at hH_4R. **a** Phenylhistamine **2** docked into the binding pocket of hH_4R; **b** dihedral angle α (CD1→CG→CB→CA) and β (CG→CB→CA→C) of $Trp^{6.48}$ during productive phase of molecular dynamic simulation of phenylhistamine **2** and Trp6.48 in its vertical and horizontal conformation as observed during molecular dynamic simulation; **c** phenylhistamine **8** docked into the binding pocket of hH_4R; **d** histaprodifen **15** docked into the binding pocket of hH_4R and dihedral angle α (CD1→CG→CB→CA) and β (CG→CB→CA→C) of $Trp^{6.48}$ during productive phase of molecular dynamic simulation of histaprodifen **15**. The amino acids of the transmembrane domains are numbered according to the nomenclature of Ballesteros et al. (2001)

Table 4 Calculated Gibbs energy of solvation for phenylhistamines **2**, **4**, **6**–**9** in water and in the binding pocket of hH_4R

cpd.	$\Delta G°_{sol}$ (L, wat)	$\Delta G°_{sol}$ (L, hH_4R)	$\Delta\Delta G°_{sol}$(water→hH_4R)
2	−204±1	−477±15	−273±16
4	−224±2	−525±11	−301±13
6	−215±2	−516±10	−301±12
7	−190±2	−512±19	−322±21
8	−205±3	−544±13	−340±16
9	−202±2	−517±19	−315±21

The calculations were performed, based on the thermodynamic integration method, using the coupling parameter λ, switching on, respectively off the interaction between ligand and surrounding, as described under "Materials and methods". $\Delta G°_{sol}$(L, wat) corresponds to the Gibbs energy of solvation of the ligand L in water, $\Delta G°_{sol}$(L, hH_4R) corresponds to the Gibbs energy of solvation of the ligand L in the binding pocket of hH_4R and $\Delta\Delta G°_{sol}$(water→hH_4R) corresponds to the change in Gibbs energy of solvation for transferring the ligand from water into binding pocket of hH_4R

histamine and $Trp^{6.48}$, an increased flexibility of $Trp^{6.48}$ was observed during the molecular dynamic simulations, compared to $Trp^{6.48}$ with histaprodifen **15** bound in the binding pocket. Representative for small phenylhistamines the evolution of the dihedral angles α (CD1→CG→CB→CA) and β (CG→CB→CA→N) of $Trp^{6.48}$, with phenylhistamine **2** in the binding pocket, during the productive phase of molecular dynamic simulation is shown. The flip, observed at about 250 ps (Fig. 4b, red box), corresponds to a conformational change of $Trp^{6.48}$ from a nearly vertical conformation into a more horizontal conformation.

The binding mode of histaprodifen **15**, based on molecular dynamic simulations, is shown in Fig. 4d. The basic amine moiety interacts electrostatically with the highly conserved $Asp^{3.32}$. The histaprodifen is embedded in a pocket, established by $Trp^{6.48}$, $Tyr^{6.51}$ and Phe168 (second extracellular loop). The neighboured Phe169 is

responsible for pharmacological differences between human and mouse H_4R (Lim et al. 2008). The highly conserved $Trp^{6.48}$ is in close contact to one of the phenyl moieties of **15**. The phenyl moieties are embedded in the binding pocket in a rigid manner. Consequently, during the molecular dynamic simulation, only a very small flexibility of $Trp^{6.48}$ was observed.

Prediction of Gibbs free energy of binding for phenylhistamines **2**, **4**, **6**–**9** In Table 4, the predicted Gibbs free energy

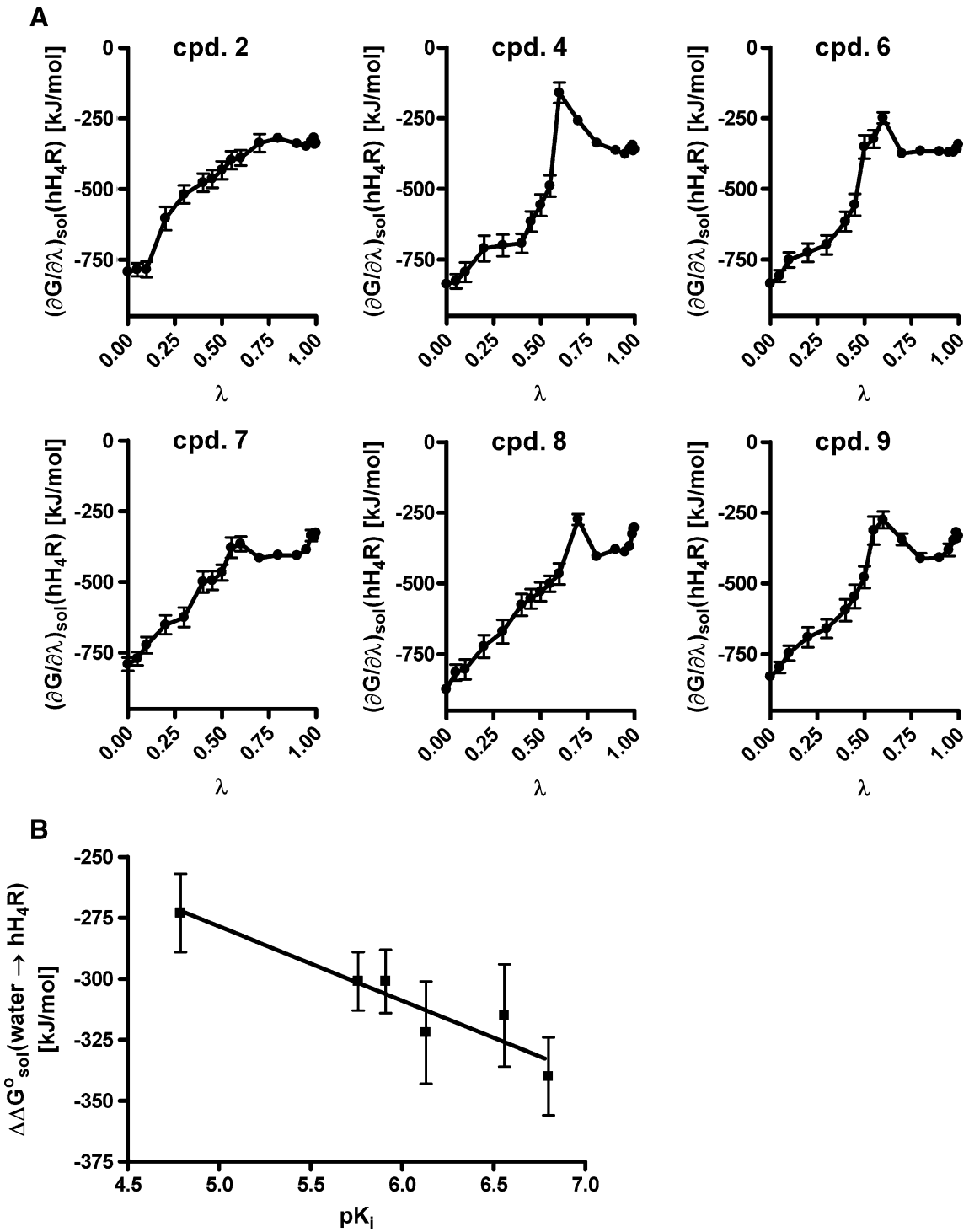

Fig. 5 Calculation of $\Delta\Delta G_{sol}(water \rightarrow hH_4R)$. **a** Evolution of Gibbs free energy of solvation $\Delta G°_{sol}(hH_4R)$ for the ligand in the binding pocket of hH_4R as a function of the coupling parameter λ, switching on, respectively off, the interaction between ligand and surrounding. **b** Predicted $\Delta\Delta G°_{sol}(water \rightarrow hH_4R)$ in correlation to experimentally determined affinities

of solvation of a ligand in water ($\Delta G°_{sol}$(water)), Gibbs free energy of solvation of a ligand in the binding pocket of hH_4R ($\Delta G°_{sol}(hH_4R)$) and the change in Gibbs free energy of solvation for transferring the ligand from the water into the binding pocket of hH_4R ($\Delta G°_{sol}(water \rightarrow hH_4R)$) are given. Additionally, in Fig. 5a, the evolution of $\Delta G°_{sol}(hH_4R)$ for representative ligands as function of the coupling parameter λ is given, whereas in Fig. 5b, the correlation between predicted $\Delta\Delta G°_{sol}(water \rightarrow hH_4R)$ and experimentally determined affinities is shown. The correlation between $\Delta\Delta G°_{sol}(water \rightarrow hH_4R)$ and the pK_i values (Fig. 5b) is given by the equation

$$\Delta\Delta G°_{sol}(water \rightarrow hH_4R) = (-126.4 \pm 32)\,kJ/mol - (30.3 \pm 5)\,kJ/mol\,pK_i$$

with r_2=0.89. Thus, the correlation between predicted $\Delta\Delta G°_{sol}(water \rightarrow hH_4R)$ and experimental affinities is very good. A comparison of the predicted slope of −30.3 kJ/mol in comparison to the theoretical value of −5.7 kJ/mol shows that the prediction is in the same range. Based on Eq. 8, the *y*-intercept, predicted to be 126.4 kJ/mol, is suggested to correspond to the change in Gibbs energy of the receptor during ligand binding.

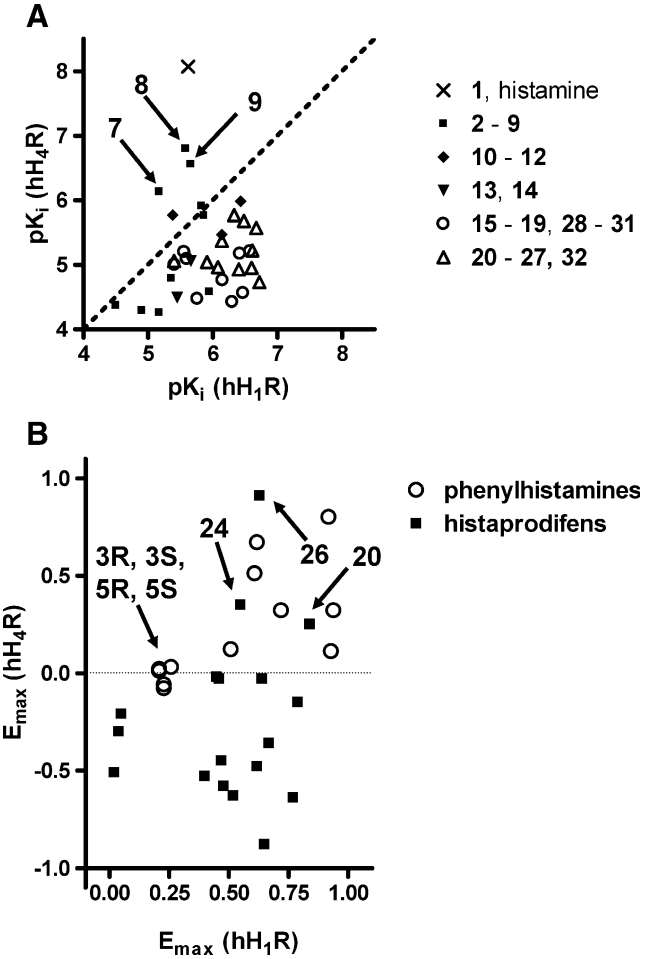

Fig. 6 Comparison of affinities and efficacies of phenylhistamines and histaprodifens between hH_1R and hH_4R. **a** Comparison of the affinities of phenylhistamines and histaprodifens between hH_4R and hH_1R (Straßer et al. 2008, 2009; Straßer and Wittmann 2010). **b** Comparison of the efficacies of phenylhistamines and histaprodifens between hH_4R and hH_1R (Straßer et al. 2008, 2009). The most important compounds are marked in the figure

Discussion

Comparison of the pharmacology of phenylhistamines, histaprodifens and phenoprodifens between hH_1R and hH_4R Figure 6 shows the correlation of the affinities of the analysed compounds at hH_1R and hH_4R. This comparison illustrates that the affinity of most of these compounds is equal to the affinities at hH_1R or lower than the affinities at hH_1R. Only the three N^{α}-methylated phenylhistamines **7**–**9** exhibit a significantly higher affinity at hH_4R than at hH_1R. It was shown previously (Schneider et al. 2010) for benzimidazole derivatives at hH_4R that the introduction of an additional methyl moiety at the basic amine leads to an increase in affinity. Thus, the phenylhistamine derivatives **7**–**9** are the first phenylhistamines exhibiting a significantly higher affinity at hH_4R, than at hH_1R (Table 2). Since the introduction of a bromine or trifluoromethyl in *meta* position of the phenyl moiety increased affinity for the small phenylhistamines **4** and **6** as well as for the N^{α}-methylated phenylhistamines **8** and **9**, we suggest that this additional small moiety fits into a small pocket of the receptor and leads to an increase in affinity due to the better ligand–receptor interaction. The same trend is observed for the same phenylhistamines at hH_1R (Straßer et al. 2009; Straßer and Wittmann 2010). The corresponding molecular modelling and molecular dynamic simulation studies revealed that the trifluoromethyl or bromine (Fig. 4a, c, arrow 2) fit into a small pocket. Thus, the pharmacological data can be explained well by molecular modelling studies. The introduction of an additional methyl group in **7**–**9**, compared to **2**, **4** and **6**, leads to a significant increase in affinity at hH_4R. In contrast, at hH_1R, this additional methyl group has no influence onto affinity. The binding data suggest that the additional methyl group stabilizes the ligand–receptor complex due to a hydrophobic interaction. The additional methyl group fits into a small pocket of hH_4R, leading to an increase in hydrophobic ligand receptor interaction on the one hand. On the other hand, the phenylhistamine is stabilized better in the binding pocket.

Besides these structural considerations, the predicted $\Delta\Delta G°_{sol}(water \rightarrow hH_4R)$ for six phenylhistamines are in very good correlation to the experimentally determined affinities (Fig. 5b). These predictions include only the

change in Gibbs energy for transfer of the ligand from the aqueous phase into the binding pocket of hH_4R, but no change in Gibbs energy due to receptor conformation. Thus, based on these results, the analysed phenylhistamines **2**, **4**, **6**–**9** may stabilize the hH_4R in similar conformations. Additionally, we predicted a change in Gibbs energy of the receptor during binding of phenylhistamines of about 126.4 kJ/mol. To the best of our knowledge, there are neither experimental nor theoretical data available in literature, which can be used for comparison. However, in future studies, further ligands, belonging to highly different ligand classes, should be analysed by a combination of molecular modelling and experimental studies, as performed in this study in order to predict the change in Gibbs energy of the receptor during ligand binding. Different ligand classes, which stabilize the receptor in different conformations, could lead to different *y*-intercepts. However, in further studies, it has to be analysed if those energetical values can be interpreted absolutely or if they have to be used relative to each other.

Histaprodifens as partial agonism–inverse agonism switch between hH_1R and hH_4R The results of the steady-state GTPase assay show that the phenylhistamines act as partial agonists at hH_1R (Straßer et al. 2009) as well as at hH_4R, except for the chiral phenylhistamines **3R**, **3S**, **5R**, **5S** and dimeric phenylhistamine **13**, which are neutral antagonists at hH_4R. In contrast, the histaprodifens exhibit partial agonism at hH_1R but inverse agonism at hH_4R. Thus, the exchange of the phenyl moiety into the phenylpropyl moiety induces a partial agonism–inverse agonism switch at hH_4R, but not at hH_1R. In general, suprahistaprodifens and phenoprodifens show partial agonism at hH_1R, but partial agonism or inverse agonism at hH_4R. Interestingly, these are the compounds which are able to bind in two different orientations into the binding pocket. Based on the results of phenylhistamines and histaprodifens, we suggest that the inverse or partial agonism of suprahistaprodifens or phenoprodifens is dependent of ligand orientation in the binding pocket. If the histaprodifen partial structure is located in the histaprodifen binding pocket, the compounds act as inverse agonists and as partial agonists otherwise. This result is very important for developing therapeutically relevant hH_4R antagonists or inverse agonists. This additional phenyl moiety decreases activity of hH_4R on the one hand, but on the other hand stimulates hH_1R, resulting in allergic reactions for example. Since histaprodifens bind to hH_1R and to hH_4R, they are not useful as therapeutics. Nevertheless, our results provide important information about structural properties to be able to construct new H_4R antagonists or dual H_1R/H_4R antagonists.

The molecular modelling studies revealed that $Trp^{6.48}$ is in close aromatic contact to one of the phenyl moieties of histaprodifen (Fig. 4d). In contrast, for the phenylhistamines, the $Trp^{6.48}$ is also in proximity to the phenylhistamine (Fig. 4a). But there is space left between the $Trp^{6.48}$ and the phenylhistamine. Thus, the $Trp^{6.48}$ can show a higher flexibility and switch between different conformations (Fig. 4b). The highly conserved $Trp^{6.48}$ is discussed to be involved in an aromatic rotamer toggle switch during receptor activation (Crocker et al. 2006). For phenylhistamines, a switch from a more vertical position, suggested to be characteristic for the inactive conformation, to a more horizontal position, suggested to be characteristic for the active conformation, could be observed in the molecular dynamic simulations (Fig. 4b, red box). However, this switch was only observed for short time scales and seemed not to be stable during the whole simulations. Nonetheless, these simulation data are in good accordance to the experimentally determined small efficacies. Thus, phenylhistamines may stabilize both the inactive and active conformation of hH_4R. Due to the close aromatic contact, the flexibility of $Trp^{6.48}$ is reduced in case of bound histaprodifen, and no conformational change, as for phenylhistamine **2**, was observed. This is in very good accordance to the experimental result that histaprodifen **15** acts as inverse agonist.

Conclusions

In this study, we identified the first phenylhistamine derivatives with a higher selectivity with regard to hH_4R than to hH_1R. This study also revealed the structural basis for the unique agonist–inverse agonist switch at histaprodifens between hH_1R and hH_4R. Thus, our study, combining experimental and modelling studies, provided important structural information for the future development of dual H_1/H_4 receptor agonists and insight into functional mechanism of receptor activation. Phenylhistamines can no longer be classified as "selective H_1R agonists".

Acknowledgements We thank A. Seefeld for performing the GTPase assays, A. Rossi and R. Winkler for performing the [^{3}H]histamine binding assays and G. Wilberg for her competent help with the cell culture. We thank B. Striegl and M. Kunze for providing the compounds **3**, **5**, **7**, **10**–**30**. We thank Prof. Schlossmann for providing infrastructure for a part of experimental studies. This work was supported by DFG (STR 1125/1-1) of the Deutsche Forschungsgemeinschaft.

References

Ballesteros JA, Shi L, Javitch JA (2001) Structural mimicry in G protein-coupled receptors: implications of the high-resolution structure of rhodopsin for structure-function analysis of rhodopsin-like receptors. Mol Pharmacol 60:1–19

Cheng Y, Prusoff WH (1973) Relationship between the inhibition constant (K_i) and the concentration of inhibitor which causes 50 per cent inhibition (I_{50}) of an enzymatic reaction. Biochem Pharmacol 22:3099–3108

Crocker E, Eilers M, Ahuja S, Hornak V, Hirshfeld A, Sheves M, Smith SO (2006) Location of Trp265 in metarhodopsin II: implications for the activation mechanism of the visual receptor rhodopsin. J Mol Biol 357:163–172

de Esch IJP, Thurmond RL, Jongejan A, Leurs R (2005) The histamine H_4 receptor as a new therapeutic target for inflammation. TRENDS Pharmacol Sci 26:462–469

Deml KF, Beermann S, Neumann D, Strasser A, Seifert R (2009) Interactions of histamine H_1-receptor agonists and antagonists with the human histamine H_4-receptor. Mol Pharmacol 76:1019–1030

Elz S, Kramer K, Pertz HH, Detert H, ter Laak AM, Kühne R, Schunack W (2000) Histaprodifens: synthesis, pharmacological *in vitro* evaluation, and molecular modeling of a new class of highly active and selective histamine H_1-receptor agonists. J Med Chem 43:1071–1084

Foord SM, Bonner TI, Neubig RR, Rosser EM, Pin JP, Davenport AP, Spedding M, Harmar AJ (2005) International Union of Pharmacology. XLVI. G protein-coupled receptor list. Pharmacol Rev 57:279–288

Hashimoto T, Harusawa S, Araki L, Zuiderveld OP, Smit MJ, Imazu T, Takashima S, Yamamoto Y, Sakamoto Y, Kurihara T, Leurs R, Bakker RA, Yamatodani A (2003) A selective human H_4-receptor agonist: (−)-2-cyano-1-methyl-3-{(2R,5R)-5-[1*H*-imidazol-4(5)-yl] tetrahydrofuran-2-yl}methylguanidine. J Med Chem 46:3162–3165

Igel P, Schneider E, Schnell D, Elz S, Seifert R, Buschauer A (2009) N^G-Acylated imidazolylpropylguanidines as potent histamine H_4 receptor agonists: selectivity by variation of the N^G-substituent. J Med Chem 52:2623–2627

Jablonowski JA, Grice CA, Chai W, Dvorak CA, Venable JD, Kwok AK, Ly KS, Wei J, Baker SM, Desai PJ, Jiang W, Wilson SJ, Thurmond RL, Karlsson L, Edwards JP, Lovenberg TW, Carruthers NI (2003) The first potent and selective non-imidazole human histamine H_4 receptor antagonist. J Med Chem 46:3957–3960

Kelley MT, Bürckstümmer T, Wenzel-Seifert K, Dove S, Buschauer A, Seifert R (2001) Distinct interaction of human and guinea pig histamine H_2-receptor with guanidine-type agonists. Mol Pharmacol 60:1210–1225

Leschke C, Elz S, Garbarg M, Schunack W (1995) Synthesis and histamine H_1 receptor agonist activity of a series of 2-phenylhistamines, 2-heteroarylhistamines, and analogues. J Med Chem 38:1287–1294

Lim HD, van Rijn RM, Ling P, Bakker RA, Thurmond RL, Leurs R (2005) Evaluation of histamine H_1-, H_2-, and H_3-receptor ligands at the human histamine H_4 receptor: identification of 4-methylhistamine as the first potent and selective H_4 receptor agonist. J Pharm Exp Ther 314:1310–1321

Lim HD, Jongejan A, Bakker RA, Haaksma E, de Esch IJP, Leurs R (2008) Phenylalanine 169 in the second extracellular loop of the human histamine H_4 receptor is responsible for the difference in agonist binding between human and mouse H_4 receptors. J Pharmacol Exp Ther 327:88–96

Menghin S, Pertz HH, Kramer K, Seifert R, Schunack W, Elz S (2003) N^α-Imidazolylalkyl and pyridylalkyl derivatives of histaprodifen: synthesis and in vitro evaluation of highly potent histamine H_1-receptor agonists. J Med Chem 46:5458–5470

Oostenbrink C, Villa A, Mark AE, van Gunsteren WF (2004) A biomolecular force field based on the free enthalpy of hydration and solvation: the GROMOS force-field parameter sets 53A5 and 53A6. J Comput Chem 25:1656–1676

Preuss H, Ghorai P, Kraus A, Dove S, Buschauer A, Seifert R (2007) Point mutations in the second extracellular loop of the histamine H_2 receptor do not affect the species-selective activity of guanidine-type agonists. Naunyn-Schmiedeberg's Arch Pharmacol 376:253–264

Scheerer P, Park JH, Hildebrand PW, Kim YJ, Krauss N, Choe HW, Hofmann KP, Ernst OP (2008) Crystal structure of opsin in its G-protein-interacting conformation. Nature 455:497–503

Schneider EH, Schnell D, Papa D, Seifert R (2009) High constitutive activity and a G-protein-independent high-affinity state of the human histamine H4-receptor. Biochemistry 48:1424–1438

Schneider EH, Strasser A, Thurmond RL, Seifert R (2010) Structural requirements for inverse agonism of indole-, benzimidazol- and thienopyrrole derived histamine H_4R ligands. J Pharmacol Exp Ther 334:513–521

Schuettelkopf AW, van Allten DMF (2004) PRODRG—a tool for high-throughput crystallography of protein–ligand complexes. Acta Cryst D60:1355–1363

Seifert R, Wenzel-Seifert K, Bürckstümmer T, Pertz HH, Schunack W, Dove S, Buschauer A, Elz S (2003) Multiple differences in agonist and antagonist pharmacology between human and guinea pig histamine H_1-receptor. J Pharmacol Exp Ther 305:1104–1115

Smits RA, de Esch IJP, Zuiderveld OP, Broeker J, Sansuk K, Guaita E, Coruzzi G, Adami M, Haaksma E, Leurs R (2008) Discovery of quinazolines as histamine H_4 receptor inverse agonists using a scaffold hopping approach. J Med Chem 51:7855–7865

Smits RA, Leurs R, de Esch IJP (2009) Major advances in the development of histamine H4 receptor ligands. Drug Discovery Today 14:745–753

Van der Spoel D, Lindahl E, Hess B, Groenhof G, Mark AE, Berendsen HJC (2005) GROMACS: fast, flexible, and free. J Comput Chem 26:1701–1718

Straßer A, Striegl B, Wittmann H-J, Seifert R (2008) Pharmacological profile of histaprodifens at four recombinant histamine H_1 receptor species isoforms. J Pharmacol Exp Ther 324:1–12

Straßer A, Wittmann HJ, Kunze M, Elz S, Seifert R (2009) Molecular basis for the selective interaction of synthetic agonists with the human histamine H_1-receptor compared with the guinea pig H_1-receptor. Mol Pharmacol 75:1–12

Straßer A, Wittmann HJ (2010) 3D-QSAR CoMFA study to predict orientation of suprahistaprodifens and phenoprodifens in the binding pocket of four histamine H_1-receptor species. Mol Inf 29:333–341

Straatsma TP, Mc Cammon JA (1991) Multiconfiguration thermodynamic integration. J Chem Phys 95:1175–1188

Terzioglu N, van Rijn RM, Bakker RA, De Esch IJP, Leurs R (2004) Synthesis and structure–activity relationships of indole and benzimidazole piperazines as histamine H_4 receptor antagonists. Bioorg & Med Chem Lett 14:5251–5256

Thurmond RL, Gelfand EW, Dunford PJ (2008) The role of histamine H_1 and H_4 receptors in allergic inflammation: the search for new antihistamines. Nature Reviews Drug Discovery 7:41–53

Thurmond RL, Desai PJ, Dunford PJ, Fung-Leung WP, Hofstra CL, Jiang W, Nguyen S, Riley JP, Sun S, Williams KN, Edwards JP, Karlsson L (2004) A potent and selective histamine H_4 Receptor antagonist with anti-inflammatory properties. J Pharmacol Exp Ther 309:404–413

Venable JD, Cai H, Chai W, Dvorak CA, Grice CA, Jablonowski JA, Shah CR, Kwok AK, Ly KS, Pio B, Wei J, Desai PJ, Jiang W, Nguyen S, Ling P, Wilson SJ, Dunford PJ,

Thurmond RL, Lovenberg TW, Karlsson L, Carruthers NI, Edwards JP (2005) Preparation and biological evaluation of indole, benzimidazole, and thienopyrrole piperazine carboxamides: potent human histamine H_4 antagonists. J Med Chem 48:8289–8298

Villa A, Mark AE (2002) Calculation of the free energy of solvation for natural analogs of amino acid side chains. J Comput Chem 23:548–553

Seifert R, Wenzel-Seifert K, Lee TW, Gether U, Sanders-Bush E, Kobilka BK (1998) Different effects of $G_{s\alpha}$ splice variants on β_2-adrenoreceptor-mediated signaling: the β_2-adrenoreceptor coupled to the long splice variant of $G_{s\alpha}$ has properties of a constitutively active receptor. J Biol Chem 273:5109–5116

Wenzel-Seifert K, Seifert R (2000) Molecular analysis of β_2-adrenoceptor coupling to G_s-, G_i-, and G_q-proteins. Mol Pharmacol 58:954–966